

Charge transfer statistics and entanglement in normal-quantum dot-superconductor hybrid structures

H. Soller and A. Komnik¹

¹*Institut für Theoretische Physik, Ruprecht-Karls-Universität Heidelberg,
Philosophenweg 19, D-69120 Heidelberg, Germany*

(Dated: January 28, 2011)

We analyze the full counting statistics (FCS) of a single-site quantum dot coupled to multiple metallic electrodes in the normal state and a superconductor for arbitrary transmission. We present an analytical solution of the problem taking into account the full energy dependence of the transmission coefficient. We identify two transport processes as sources of entanglement between the current carriers by observing positive cross current correlations. Furthermore, we consider ferromagnetic electrodes and show how they can be used as detectors in experiments violating the Bell-Clauser-Horne-Shimony-Holt inequality.

PACS numbers: 73.21.La, 72.70.+m 73.23.-b

Correlations represent one of the main ingredients of quantum mechanics. They may persist even if the particles are causally disconnected which allows for experimental Bell inequality tests, quantum cryptography and quantum teleportation¹. In quantum optics using e. g. parametric downconversion² many interesting experiments investigating the fundamentals of quantum mechanics became possible³. Solid state entanglers have only recently been shown to work experimentally using a superconducting finger coupled to normal leads directly⁴⁻⁶ or via two quantum dots^{7,8}. They rely on the non-local or crossed Andreev reflection (CAR) in multi-terminal structures with a superconducting lead where an incident electron from one of the electrodes is reflected by the superconductor into another electrode. This process produces entanglement between the current carriers in the two leads since the correlations of the spin singlet (Cooper pair) are transferred to the spatially separated electrons. The nature of CAR has been investigated further using ferromagnetic contacts^{9,10}. Recently, the nonlocal conductance in superconductor hybrid structures has been extensively studied theoretically using different approaches¹¹⁻¹⁸. On the one hand the conductance properties of interacting quantum dots with a superconducting lead have been discussed^{7,19-21}. On the other hand the full counting statistics (FCS) of multi-terminal systems with a chaotic cavity and a superconducting connector were investigated²²⁻²⁶. Among other things the cross-correlation noise has been found to be an efficient tool for discrimination of the current caused by CAR from other current contributions²⁷⁻³⁵.

Even in its basic realization the noninteracting quantum dot usually shows a highly nonlinear transmission leading to nonlinear current-voltage relations. Combined with a superconducting electrode, the single-particle density of states of which is itself highly nonlinear due to the finite gap, the resulting structure is expected to possess transport properties with a nontrivial voltage dependence. Thus far these aspects have not been fully

taken into account. In this paper we would like to close this gap by considering a quantum dot modelled by a noninteracting resonant level. This setup enables one to access the full energy dependence of transmission characteristics generated by the superconducting density of states (DOS) as well as by the energy-dependent transmission of the dot.

The quantity of our primary interest is the FCS in terms of the cumulant generating function (CGF) χ . It represents a very convenient tool for the calculation of a variety of transport properties. It is directly related to the probability distribution $P(Q)$ to transfer Q elementary charges during a fixed very long measurement time τ . By a simple derivation with respect to some parameters (counting fields) χ gives all cumulants (irreducible momenta) of $P(Q)$ ^{36,37}. The relevance of higher order cumulants has been recently demonstrated experimentally^{38,39}. Moreover, the analytic structure of the CGF provides deep insights into the different transport processes⁴⁰⁻⁴⁴. As we shall demonstrate later, in the case of the multi-terminal quantum dot considered here, the FCS will reveal the different facets of entanglement that we expect to be observable in upcoming experiments.

The Hamiltonian for the system under consideration is given by

$$H = H_0 + H_d + H_T + H_s. \quad (1)$$

The term H_0 describes normal or ferromagnetic electrodes in the language of the respective electron field operators $\Psi_{\alpha\sigma}(x)$, where $\alpha = 1, \dots, N$ numbers the electrodes. The local density of states $\rho_{0\alpha}$ in the leads is assumed to be very weakly energy dependent in the relevant range of energies. The normal electrodes are modelled by noninteracting fermionic continua held at the chemical potentials μ_α . Ferromagnetic electrodes are described by the Stoner model with an exchange energy h_{ex}

as in⁴⁵

$$H_{\text{Stoner},\alpha} = \sum_{k,\sigma} \epsilon_k \Psi_{k\alpha\sigma}^+ \Psi_{k\alpha\sigma} - h_{\text{ex},\alpha} \sum_k (\Psi_{k\alpha\uparrow}^+ \Psi_{k\alpha\uparrow} - \Psi_{k\alpha\downarrow}^+ \Psi_{k\alpha\downarrow}).$$

Consequently they can be described as fermionic continua with a spin-dependent DOS $\rho_{0\sigma\alpha} = \rho_{0\alpha}(1 + \sigma P_\alpha)$, where P_α is the polarization⁴⁵. The superconducting electrode is described by the BCS Hamiltonian with the gap Δ of the superconducting terminal⁴⁶

$$H_s = \sum_{k,\sigma} \epsilon_k \Psi_{ks\sigma}^+ \Psi_{ks\sigma} + \Delta \sum_k (\Psi_{ks\uparrow}^+ \Psi_{-ks\downarrow}^+ + \Psi_{-ks\downarrow} \Psi_{ks\uparrow}).$$

The superconductor is kept in equilibrium as in previous treatments of similar problems⁴¹. The applied bias voltages are given by $V_\alpha = \mu_s - \mu_\alpha = -\mu_\alpha$ (we use units where $e = \hbar = k_B = 1$). The electron exchange between the dot and the electrodes is given by⁴⁷

$$H_T = \sum_{\alpha,\sigma} \gamma_\alpha [d_\sigma^+ \Psi_{\alpha\sigma}(x=0) + h.c.] + \sum_\sigma \gamma_s [d_\sigma^+ \Psi_{s\sigma}(x=0) + h.c.],$$

where γ_α or γ_s are the tunneling amplitudes between the dot and the normal or superconducting electrodes. The tunneling is assumed to be local and to occur at $x = 0$ in the coordinate system of the respective electrode. d_σ is the annihilation operator of an electron with spin σ on

the dot. The quantum dot in the presence of a magnetic field B is modelled by $H_d = \sum_\sigma (\Delta_d + \sigma h/2) d_\sigma^+ d_\sigma =: \sum_\sigma \delta_\sigma d_\sigma^+ d_\sigma$, where Δ_d is the bare dot energy and in SI-units $h = \mu_B g B$ with Bohr's magneton μ_B and the gyromagnetic ratio g ⁴⁸.

In order to determine the FCS we calculate the CGF $\ln \chi(\boldsymbol{\lambda}) = \ln \langle e^{i\lambda Q} \rangle$, which depends on the counting fields $\boldsymbol{\lambda} = (\lambda_1, \dots, \lambda_N, \lambda_s)$ in the respective electrodes. It provides all the higher statistical moments (or irreducible cumulants) $\langle\langle Q^n \rangle\rangle$ of $P(Q)$. The CGF is calculated using the Keldysh Green's function approach^{36,49} adapted to quantum impurity problems in^{50–52}. According to the generalized Keldysh approach one obtains for the CGF⁴⁰

$$\chi(\boldsymbol{\lambda}) = \langle T_C \exp \left[-i \int_C dt H_T^{\lambda(t)} \right] \rangle,$$

where the dependence on the counting fields is contained in

$$H_T^{\lambda(t)} = \sum_{\alpha,\sigma} \gamma_\alpha \left[e^{i\lambda_\alpha(t)/2} d_\sigma^+ \Psi_{\alpha\sigma}(x=0) + h.c. \right] + \sum_\sigma \gamma_s \left[e^{i\lambda_s(t)/2} d_\sigma^+ \Psi_{s\sigma}(x=0) + h.c. \right].$$

The different counting fields are nonzero only during the measurement time τ and have different signs on the forward and backward path of the Keldysh contour. The scattering matrix has two energy regimes⁵³ with energy-dependent transmission coefficients. The respective Fermi distributions of the individual terminals are abbreviated by n_α and $n_{\alpha+} := 1 - n_\alpha(-\omega)$ for hole-like contributions. This allows to express the CGF in the form given in equation (2).

$$\begin{aligned} \ln \chi(\boldsymbol{\lambda}) = & \frac{\tau}{\pi} \int d\omega \left[\theta \left(\frac{|\omega| - \Delta}{\Delta} \right) \left(\sum_\sigma \ln \left\{ 1 + \sum_{i,j=1,\dots,N,s, i \neq j} T_{ij\sigma}(\omega) n_i (1 - n_j) (e^{i(\lambda_i - \lambda_j)} - 1) \right\} \right) \right. \\ & + \frac{1}{2} \theta \left(\frac{\Delta - |\omega|}{\Delta} \right) \left(\sum_\sigma \ln \left\{ \left[1 + \sum_{i,j=1,\dots,N, i \neq j} T_{Aij\sigma} n_i (1 - n_j) (e^{i(\lambda_i - \lambda_j)} - 1) \right] \right. \right. \\ & \times \left[1 + \sum_{i,j=1,\dots,N, i \neq j} T_{Aij\sigma h} n_{j+} (1 - n_{i+}) (e^{i(\lambda_i - \lambda_j)} - 1) \right] + \sum_{i=1,\dots,N} T_{Ais} \left[n_i (1 - n_{i+}) (e^{2i(\lambda_i - \lambda_s)} - 1) \right] \\ & \left. \left. + \sum_{i,j=1,\dots,N, i \neq j} T_{CAij\sigma} \left[n_{j+} (1 - n_i) (e^{i(2\lambda_s - \lambda_i - \lambda_j)} - 1) + n_i (1 - n_{j+}) (e^{-i(2\lambda_s - \lambda_i - \lambda_j)} - 1) \right] \right\} \right], \quad (2) \end{aligned}$$

where we define

$$T_{ij\sigma}(\omega) = 4\Gamma_i \Gamma_j (1 + \sigma P_i) (1 + \sigma P_j) / [(\omega - \delta_\sigma)^2 + (\sum_{k=1,\dots,N} \Gamma_k (1 + \sigma P_k) + \Gamma_{s1})^2], \text{ with } (P_s = 0) \quad (3)$$

$$T_{Aij\sigma e} = 4\Gamma_i (1 + \sigma P_i) \Gamma_j (1 + \sigma P_j) \{(\omega - \delta_{-\sigma})^2 + [\sum_{k=1,\dots,N} \Gamma_k (1 - \sigma P_k)]^2\} / \det_{A\sigma}(\omega), \quad (4)$$

$$T_{Aij\sigma h} = 4\Gamma_i(1-\sigma P_i)\Gamma_j(1-\sigma P_j)\{(\omega-\delta_\sigma)^2 + [\sum_{k=1,\dots,N}\Gamma_k(1+\sigma P_k)]^2\}/\det_{A\sigma}(\omega), \quad (5)$$

$$T_{Ai\sigma} = 4\Gamma_i^2(1-\sigma P_i)(1+\sigma P_i)\Gamma_{s2}^2/\det_{A\sigma}(\omega), \quad T_{CAij\sigma} = 4\Gamma_i(1+\sigma P_i)\Gamma_j(1-\sigma P_j)\Gamma_{s2}^2/\det_{A\sigma}(\omega), \quad (6)$$

$$\begin{aligned} \det_{A\sigma}(\omega) = & (\omega-\delta_\sigma)^2(\omega-\delta_{-\sigma})^2 + \{[\sum_{k=1,\dots,N}\Gamma_k(1+\sigma P_k)]^2 + \Gamma_{s2}^2\} \\ & \times \{[\sum_{k=1,\dots,N}\Gamma_k(1-\sigma P_k)]^2 + \Gamma_{s2}^2\} + [\sum_{k=1,\dots,N}\Gamma_k(1+\sigma P_k)]^2(\omega-\delta_{-\sigma})^2 \\ & + [\sum_{k=1,\dots,N}(1-\sigma P_k)]^2(\omega-\delta_\sigma)^2 + 2\Gamma_{s2}^2(\omega-\delta_\sigma)(\omega-\delta_{-\sigma}), \end{aligned} \quad (7)$$

The abbreviation $\Gamma_i = \pi\rho_{0i}|\gamma_i|^2/2$ is the (energy-independent) dot-lead contact transparency with dimension energy for the normal leads. For the superconducting leads it is affected by the energy-dependent superconducting DOS so that

$$\Gamma_{s1} = \pi\rho_{0s}|\gamma_s|^2|\omega|/(2\sqrt{\omega^2-\Delta^2}) \quad (8)$$

$$\Gamma_{s2} = \pi\rho_{0s}|\gamma_s|^2\Delta/(2\sqrt{\Delta^2-\omega^2}). \quad (9)$$

For $|\omega| > \Delta$ the counting factors $e^{i(\lambda_i-\lambda_j)}$ describe single electron transport between the different terminals. For $|\omega| < \Delta$ the superconducting DOS only allows excitations from the Cooper pair condensate which leads to different transport characteristics. They are described by counting factors $e^{2i(\lambda_s-\lambda_i)}$ and $e^{2i\lambda_s-i\lambda_i-i\lambda_j}$ referring to the transfer of two particles from the superconductor to a single or two separate terminals. The transmission coefficients $T_{Ai\sigma}$ and $T_{CAij\sigma}$ therefore refer to Andreev-reflection and CAR respectively.

For $\Delta \rightarrow 0$ the CGF reduces to the well-known expression for the CGF of a noninteracting dot in a multi-terminal geometry⁴⁴. The same holds for $\gamma_s \rightarrow 0$.

The FCS for a three-terminal structure at $T = 0$ using a chaotic cavity with energy-independent transmission instead of a resonant level have been calculated before^{22,26}. In this case the CGF adopts a characteristic double square root form. The first square root instead of a logarithm is due to the diffusive transport through a chaotic cavity⁵⁴. The second square root may be explained looking at physical observables that are calculated via derivatives of the CGF, where it leads to additional factors 1/2. Therefore it corresponds to the factors 1/2 in the transparencies Γ_i , Γ_{s1} and Γ_{s2} that are due to the separate treatment of electrons and holes as a consequence of the proximity effect. The transmission coefficients are different in our case because of the energy-dependent DOS of the quantum dot. As in our case the ones for single electron transmission, direct Andreev reflection and crossed Andreev reflection are proportional to $\Gamma_1\Gamma_2$, $(\Gamma_1^2 + \Gamma_2^2)\Gamma_s^2$ and $2\Gamma_1\Gamma_2\Gamma_s^2$, respectively.

Considering the case of only a single normal electrode the conductivity at low voltages and no magnetic field is

given by

$$\begin{aligned} G_{NQS} = & 4 T_{A1\uparrow}|_{h=0, \omega=0}, \\ = & \frac{4e^2}{h} \left(\frac{2\tilde{\Gamma}_1\tilde{\Gamma}_s}{4\Delta_d^2 + \tilde{\Gamma}_1^2 + \tilde{\Gamma}_s^2} \right). \end{aligned}$$

In the last step we introduced $\tilde{\Gamma}_1 = 2\Gamma_1$, $\tilde{\Gamma}_s = 2\Gamma_s$ and restored SI-units. The result coincides with the one previously obtained in⁵⁵.

The three-terminal case with two normal metal drains is of particular interest. Positive cross correlations between the normal electrodes can be used to probe the existence of entanglement²⁵. Along with the noise the cross correlation can be calculated as a second derivative of the CGF

$$P_{12}^I = -\frac{1}{\tau} \left. \frac{\partial^2 \ln \chi(\lambda, \tau)}{\partial \lambda_1 \partial \lambda_2} \right|_{\lambda=0}.$$

Depending on the coupling and voltages choice different cross correlations may be observed. Three different types of transport between the normal drains are present: the direct single electron current proportional to $\Gamma_1\Gamma_2(V_1 - V_2)$, the direct Andreev reflections (DA) proportional to $2(\Gamma_1^2 V_1 + \Gamma_2^2 V_2)\Gamma_s^2$ or CAR proportional to $2\Gamma_1\Gamma_2\Gamma_s^2(V_1 + V_2)$. If the superconducting terminal is weakly coupled to the quantum dot, cross correlations will either be dominated by single electron transmission or, for $V_1 \approx V_2$, by direct Andreev reflections to a normal drain leading to negative correlations. There are two cases in which positive cumulants are observed. If the superconductor is coupled better to the quantum dot than the normal terminals, positive correlations may be observed for voltages close to the superconducting gap and $V_1 \approx -V_2$, see Figure 1. In this case CAR is strongly suppressed and one expects single electron transmission to be dominant. However, the energy-dependent DOS of the superconductor leads to large transmission coefficients for double Andreev reflections from one normal drain to the superconductor and further to the second normal electrode.

This Andreev-reflection Enhanced Transmission (AET) is also observed if an additional broadening of the BCS DOS is taken into account as in¹², where $\omega \rightarrow \omega + i\eta_s$ with

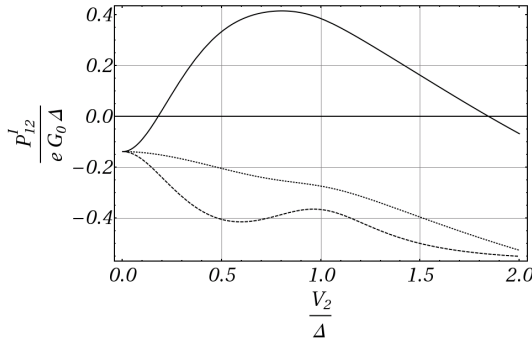


FIG. 1: Cross Correlations P_{12}^I calculated from the CGF in equation (2) with the parameters $\Gamma_s = \Delta/2 = \Gamma_1$, $\Gamma_2 = 0.2\Delta$, $\Delta_d = 0$, $T = 0.1\Delta$ as a function of V_2 for $V_1 = -V_2$ (solid line), $V_1 = 0$ (dotted line) and $V_1 = V_2$ (dashed line). The three cuts show that one observes negative cross correlation for $V_1 = V_2$ and $V_1 = 0$ whereas a positive cross correlation maximum for $V_1 = -V_2$ close to the superconducting gap caused by AET is obtained.

a typical experimental value η_s of about $10^{-2}\Delta$. AET is a robust phenomenon. In modern experiments using either InAs nanowires⁸ or carbon nanotubes⁷ $\Gamma_s \approx \Delta$ is generically obtained. The hybridisation with the normal leads can be tuned via top gates to e.g. $\Gamma_n \approx \Gamma_s/2$. AET should then be observable via cross correlations or from the direct currents.

The second case for positive correlations is observed for strong coupling of the superconductor to the quantum dot and asymmetrically coupled normal terminals. Since the contribution by CAR is proportional to $V_1 + V_2$ a voltage bias may be applied via the the weakly coupled normal electrode $j = 1, 2$. The DA contribution is proportional to Γ_j^2 and therefore will be strongly suppressed for this weakly coupled drain. For voltages well below the gap CAR dominates over single electron transmission because a CAR is possible in two ways. In Figure 2 we show the cross correlation in this situation.

The directions of the currents are different in the case of CAR and AET. CAR describes electron transfer into/from the superconductor whereas in the case of AET the superconductor only assists electron transfer between the normal drains. The FCS formalism allows us to follow the different transport processes independently. In the case of CAR two electrons from the same Cooper pair are transferred to spatially separate electrodes. In the case of AET an electron impinging on the superconductor is retroreflected as a hole. The same Cooper pair that was generated by this Andreev reflection is then transferred further by a hole from the second normal drain that is retroreflected as an electron. In the case of CAR we therefore observe entangled electrons in the normal electrodes both in energy and spin space. Considering AET the electron and the hole originate from one Cooper pair and due to the conservation of spin and energy must also be entangled in energy and spin space. Only AET and CAR generate positive correlations which therefore

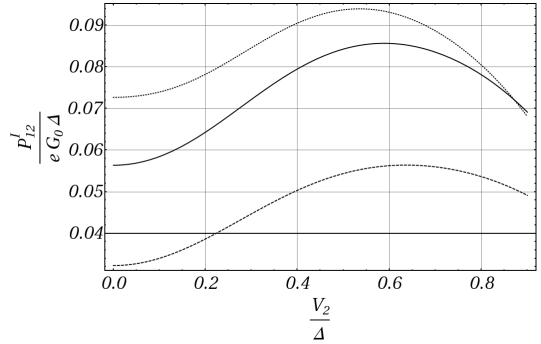


FIG. 2: Cross correlation P_{12}^I calculated from the CGF in equation (2) with the parameters $\Gamma_s = \Delta$, $\Gamma_1 = 0.4\Delta$, $\Delta_d = 0$, $T = 0.1\Delta$, $V_1 = 0$ as a function of V_2 . The dotted line shows the result for $\Gamma_2 = 0.05\Delta$, the solid line is for $\Gamma_2 = 0.1\Delta$ and the dashed line is for $\Gamma_2 = 0.15\Delta$. Consequently the second electrode is weakly coupled. Therefore the CAR processes dominate for voltages below the gap over single electron transmission and DA leading to a positive cross correlation. This effect is enhanced for weaker coupling of the second electrode. The effect is also present at finite V_1 but it is weakened.

indicate the presence of entanglement.

The asymmetric coupling necessary to observe CAR can easily be realized experimentally by fabricating a simple NQS structure on a substrate with a single normal drain and using an STM tip as the second weakly coupled terminal.

There are two further possibilities to observe CAR as the dominant transport channel. On the one hand using additional normal drains enhances the possibilities for CAR as can be seen directly from the CGF in equation (2). The combinatorical factor naturally leads to a dominance of CAR. On the other hand DA and single electron transmission can be fully suppressed by ferromagnetic drains with antiparallel polarisation²⁵. In this case we always observe positive correlations for voltages below the gap and not too high temperatures if the polarisations are chosen strong enough. For $P_1 = -P_2 = 1$ we also considered the case of three normal terminals and we obtained $P_{12}^I = 0$ in accordance with previous calculations⁵⁶.

A ferromagnet preferably accepts electrons of a specific spin. It may therefore also be viewed as a detector for this specific spin direction^{25,56}. This fact enables us to demonstrate a possible violation of the Bell-Clauser-Horne-Shimony-Holt inequality along the lines of^{25,56}. First we have to include the spatial direction of magnetization into our previous treatment, where we only considered one specific quantization axis for the polarizations of the ferromagnet.

We consider a device as in Figure 3 with four F_n ($n = 1, \dots, 4$) terminals. The drains F_1, F_2 and F_3, F_4 are pairwise polarized in opposite directions to serve as spin detectors. First we only consider the case with a single quantum dot in the middle. For a simplified discussion we want to consider the special case $P_1 = -P_2 =$

$P_3 = -P_4$ and $\Gamma_1 = \Gamma_2$, $\Gamma_3 = \Gamma_4$ as in⁵⁶. To avoid confusion with the different quantization axes we limit our discussion to $h = 0$. The energy-dependent transmission coefficients for CAR in the case of four ferromagnetic drains and $\alpha = 1, 2$, $\beta = 3, 4$ are given by $T_{CA\alpha\beta\sigma} = 4\Gamma_1\Gamma_3(1 - P_1P_3)\Gamma_{s2}^2/\det_{A\sigma}(\omega)$. The polarization in the direction-dependent case may be rewritten as $P_i \rightarrow \mathbf{g}_i = P_i\mathbf{m}_i$, $i = 1, 3$ with a unit vector \mathbf{m}_i describing the magnetization direction⁵⁷. In this way we obtain the transmission coefficients $T_{CA\alpha\beta\sigma} = 4\Gamma_1\Gamma_3(1 - \mathbf{g}_\alpha\mathbf{g}_\beta)\Gamma_{s2}^2/\det_{A\sigma}(\omega)$. The differential conductances at $T = 0$ for the respective crossed Andreev reflections to drain α and β can be directly read off via $G_{CA\alpha\beta\sigma} = \frac{4}{2\pi} [T_{CA\alpha\beta\sigma}(V) + T_{CA\alpha\beta\sigma}(-V)]$. As CAR is a nonlocal process these conductances describe nonlocal correlations.

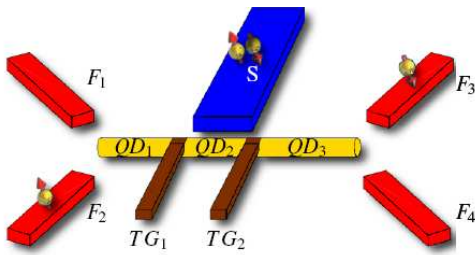


FIG. 3: Schematic setup for demonstrating the violation of Bell's inequality. A nanowire is connected to four ferromagnetic drains $F_{1,\dots,4}$ and a superconductor S . The top gates $TG_{1,2}$ may be used to divide the nanowire into three quantum dots $QD_{1,2,3}$ with tunable coupling.

They also give the probabilities $p_{\alpha,\beta}$ for simultaneous detection of an electron at α and β by

$$p_{\alpha,\beta} = G_{CA\alpha\beta\sigma} / \sum_{\{\gamma,\delta\}} G_{CA\gamma\delta\sigma}. \quad (10)$$

The drains 1, 2 and 3, 4 represent spin detectors (Alice, Bob) with respect to two possible choices for the direction $\mathbf{g}_{1,3}$, $\mathbf{g}'_{1,3}$. The spins can be detected by the respective currents. We shall discard events with both electrons going to the same detector by normalizing the probabilities to go to different detectors as in⁵⁶.

We should stress that we need to record every single event separately. To go over to a non-time-resolved measurement scheme one needs to observe not just the spin current but the spin-current fluctuations⁵⁸.

As in^{25,56} we find for the Bell parameter $\epsilon = |\mathbf{g}_1\mathbf{g}_3 + \mathbf{g}'_1\mathbf{g}_3 + \mathbf{g}'_1\mathbf{g}'_3 - \mathbf{g}_1\mathbf{g}'_3|$. The maximum of ϵ is $2\sqrt{2}$. Bell's inequality $\epsilon \leq 2$ is violated if the polarization $\|\mathbf{g}_1\| = P_1 = P_3 \geq 2^{-\frac{1}{4}}$ as in other treatments⁵⁹. Such a degree of polarization is hard to obtain with ferromagnets but may easily be reached using double-quantum dot structures⁶⁰. This also represents a direct measurement of the concurrence (C) since the maximal value of the Bell parameter $\epsilon_{max} = 2\sqrt{1 + C^2}$, where C is a measure of entanglement

with possible values between 0 and 1.

The same expression for the Bell parameter has been obtained previously by Morten et al.²⁵ for a chaotic cavity. Our result shows that the concurrence does not depend on how the beam splitter geometry is realized. The cross correlation however is affected by the difference in the transmission coefficients and therefore only indicates the presence of entanglement. The described experiment appears to be a perfect analogue to the optical experiments using parametric downconversion². However, care has to be taken with respect to the distinguishability of particles. In optical experiments one detects spatially separated particles where entanglement is unambiguously defined. In the case of a single quantum dot we detect the spin direction of electrons coming from the dot which are indistinguishable. In this situation the state has the form of a single Slater determinant, which is considered a nonentangled state⁶¹. But we can easily go over to the distinguishable case by using the full power of the experimental setup in Figure 3. By tuning the top gate voltages one can induce tunnel barriers to obtain a triple quantum dot in series⁶². If we go over to a strongly coupled triple dot we obtain well separated densities of states and therefore detect distinguishable particles from QD_1 or QD_3 . In this case we can neglect resonant tunneling and evaluate the transmission coefficients by multiplying the transmissions through the different quantum dots. In this situation we also obtain the same Bell parameter, however now for an unambiguously entangled state. The correlations remain the same in the distinguishable or indistinguishable case.

To conclude we have analytically calculated the full counting statistics (FCS) of a noninteracting quantum dot (resonant level) contacted by multiple metallic electrodes in the normal state as well as by a superconducting one. The superconducting ground state leads to positive cross correlations between the currents in the normal drains by two transport phenomena that we identified as crossed Andreev reflections (CAR) and Andreev-reflection enhanced transmission (AET). Our results allow for an analysis of a possible violation of the Bell-Clauwer-Horne-Shimony-Holt inequality that is related to a measurement of the concurrence C . Interestingly, we find it to be independent of the constellation of coupling parameters. Moreover, it coincides with the results found for the quantum dot realization via a chaotic cavity. Finally we discussed the question of entanglement for indistinguishable and distinguishable particles. We have shown that the correlations should be unaffected by this distinction and how both cases can be addressed experimentally.

The authors would like to thank S. Maier and P. Plötz for many interesting discussions. The financial support was provided by the DFG under grant No. 2235/3, and by the Kompetenznetz "Funktionelle Nanostrukturen III" of the Baden-Württemberg Stiftung (Germany).

¹ M. A. Nielsen and I. L. Chuang, *Quantum Computation and quantum Information and references therein* (Cambridge University Press, 2000).

² Y. H. Shih and C. O. Alley, Phys. Rev. Lett. **61**, 2921 (1988).

³ e. g. D. Bouwmeester, J.-W. Pan, K. Mattle, M. Eibl, H. Weinfurter, and A. Zeilinger, Nature **390**, 575 (1997).

⁴ J. Wei and V. Chandrasekhar, Nat. Phys. **6**, 494498 (2010).

⁵ S. Russo, M. Kroug, T. M. Klapwijk, and A. F. Morpurgo, Phys. Rev. Lett. **95**, 027002 (2005).

⁶ P. Cadden-Zimansky and V. Chandrasekhar, Phys. Rev. Lett. **97**, 237003 (2006).

⁷ L. G. Herrmann, F. Portier, P. Roche, A. L. Yeyati, T. Kontos, and C. Strunk, Phys. Rev. Lett. **104**, 026801 (2010).

⁸ L. Hofstetter, S. Csonka, J. Nygård, and C. Schönenberger, Nature **461**, 960 (2009).

⁹ D. Beckmann and H. v. Löhneysen, Appl. Phys. A **89**, 603 (2007).

¹⁰ D. Beckmann, H. B. Weber, and H. v. Löhneysen, Phys. Rev. Lett. **93**, 197003 (2004).

¹¹ G. Falci, D. Feinberg, and F. W. J. Hekking, Europhys. Lett. **54**, 255 (2001).

¹² R. Mélin and D. Feinberg, Phys. Rev. B **70**, 174509 (2004).

¹³ J. M. Byers and M. E. Flatté, Phys. Rev. Lett. **74**, 3305 (1995).

¹⁴ G. Deutscher and D. Feinberg, Appl. Phys. Lett. **76**, 487 (2000).

¹⁵ T. Yamashita, S. Takahashi, and S. Maekawa, Phys. Rev. B **68**, 174504 (2003).

¹⁶ M. S. Kalenkov and A. D. Zaikin, Phys. Rev. B **76**, 224506 (2007).

¹⁷ A. Brinkman and A. A. Golubov, Phys. Rev. B **74**, 214512 (2006).

¹⁸ P. Recher, E. V. Sukhorukov, and D. Loss, Phys. Rev. B **63**, 165314 (2001).

¹⁹ A. Levy Yeyati, F. S. Bergeret, A. Martin-Rodro, and T. M. Klapwijk, Nature Phys. **3**, 455 (2007).

²⁰ J. C. Cuevas, A. Levy Yeyati, and A. Martín-Rodero, Phys. Rev. B **63**, 094515 (2001).

²¹ A. Braggio, M. Governale, M. G. Pala, and J. Knig, Solid State Communications **151**, 155 (2011).

²² J. Börlin, W. Belzig, and C. Bruder, Phys. Rev. Lett. **88**, 197001 (2002).

²³ J. P. Morten, A. Brataas, and W. Belzig, Phys. Rev. B **74**, 214510 (2006).

²⁴ J. P. Morten, A. Brataas, and W. Belzig, Appl. Phys. A **89**, 609 (2007).

²⁵ J. P. Morten, D. Huertas-Hernando, W. Belzig, and A. Brataas, Europhys. Lett. **81**, 40002 (2008).

²⁶ J. P. Morten, D. Huertas-Hernando, W. Belzig, and A. Brataas, Phys. Rev. B **78**, 224515 (2008).

²⁷ G. Bignon, M. Houzet, F. Pistolesi, and F. W. J. Hekking, Europhys. Lett. **67**, 110 (2004).

²⁸ P. Samuelsson and M. Büttiker, Phys. Rev. Lett. **89**, 046601 (2002).

²⁹ T. Gramespacher and M. Büttiker, Phys. Rev. B **61**, 8125 (2000).

³⁰ D. Sánchez, R. López, P. Samuelsson, and M. Büttiker, Phys. Rev. B **68**, 214501 (2003).

³¹ M. P. Anantram and S. Datta, Phys. Rev. B **53**, 16390 (1996).

³² F. Taddei and R. Fazio, Phys. Rev. B **65**, 134522 (2002).

³³ J. Torrès and T. Martin, Eur. Phys. J. B **12**, 319 (1999).

³⁴ V. Bouchiat, N. Chtchelkatchev, D. Feinberg, G. B. Lesovik, T. Martin, and J. Torreš, Nanotechnology **14**, 77 (2003).

³⁵ G. B. Lesovik, T. Martin, and G. Blatter, Europ. Phys. J. B **24**, 287 (2001).

³⁶ L. S. Levitov, H. W. Lee, and G. B. Lesovik, J. Math. Phys. **37**, 4845 (1996).

³⁷ Y. V. Nazarov and M. Kindermann, Europ. Phys. J. B **35**, 413 (2003).

³⁸ B. Reulet, J. Senzier, and D. E. Prober, Phys. Rev. Lett. **91**, 196601 (2003).

³⁹ S. Gustavsson, R. Leturcq, T. Ihn, K. Ensslin, M. Reinwald, and W. Wegscheider, Phys. Rev. B **75**, 075314 (2007).

⁴⁰ L. S. Levitov and M. Reznikov, Phys. Rev. B **70**, 115305 (2004).

⁴¹ B. A. Muzykantskii and D. E. Khmelnitskii, Phys. Rev. B **50**, 3982 (1994).

⁴² H. Saleur and U. Weiss, Phys. Rev. B **63**, 201302 (2001).

⁴³ J. C. Cuevas and W. Belzig, Phys. Rev. Lett. **91**, 187001 (2003).

⁴⁴ T. L. Schmidt, A. Komnik, and A. O. Gogolin, Phys. Rev. Lett. **98**, 056603 (2007).

⁴⁵ R. Mlin, Europ. Phys. J. B **39**, 249 (2004).

⁴⁶ J. Bardeen, L. N. Cooper, and J. R. Schrieffer, Phys. Rev. **108**, 1175 (1957).

⁴⁷ M. H. Cohen, L. M. Falicov, and J. C. Phillips, Phys. Rev. Lett. **8**, 316 (1962).

⁴⁸ T. L. Schmidt, A. O. Gogolin, and A. Komnik, Phys. Rev. B **75**, 235105 (2007).

⁴⁹ Y. V. Nazarov, Ann. Phys. **8**, 193 (1999).

⁵⁰ A. O. Gogolin and A. Komnik, Phys. Rev. B **73**, 195301 (2006).

⁵¹ D. A. Bagrets, Y. Utsumi, D. S. Golubev, and G. Schön, Fortschritte der Physik **54**, 917 (2006).

⁵² T. L. Schmidt, A. Komnik, and A. O. Gogolin, Phys. Rev. B **76**, 241307 (2007).

⁵³ P. Schwab and R. Raimondi, Phys. Rev. B **59**, 1637 (1999).

⁵⁴ W. Belzig and Y. V. Nazarov, Physical Review Letters **87**, 197006 (2001).

⁵⁵ C. W. J. Beenakker, Phys. Rev. B **46**, 12841 (1992).

⁵⁶ A. Di Lorenzo and Y. V. Nazarov, Phys. Rev. Lett. **94**, 210601 (2005).

⁵⁷ D. Huertas-Hernando, Y. V. Nazarov, and W. Belzig, Phys. Rev. Lett. **88**, 047003 (2002).

⁵⁸ N. M. Chtchelkatchev, G. Blatter, G. B. Lesovik, and T. Martin, Phys. Rev. B **66**, 161320 (2002).

⁵⁹ S. Kawabata, J. Phys. Soc. Jpn. **70**, 1210 (2001).

⁶⁰ J. P. Dahlhaus, S. Maier, and A. Komnik, Phys. Rev. B **81**, 075110 (2010).

⁶¹ G. C. Ghirardi and L. Marinatto, Opt. & Spec. **99**, 386 (2005).

⁶² K. Grove-Rasmussen, H. I. Jørgensen, T. Hayashi, P. E. Lindelof, and T. Fujisawa, Nanoletters **8**, 1055 (2008).